Machine Tool Equipped with a Counter Balance Feed Drive in the Z Direction with Right and Left Ball Screws and the Influence of Anisotropic Mechanical Behavior on Small-Diameter Drilling Processes

Yusuke Nosaka*, Toshiki Hirogaki, and Eiichi Aoyama

***Abstract*—In recent years, electronic devices have become lighter, thinner, shorter, smaller, and more multifunctional, motivating micro drilling technology to become more sophisticated. To meet the demands of electronic applications, this paper proposes a drilling machine tool with a counterbalance vibration control mechanism. In this report, focusing on the timing of table feed rate changes during drilling, drilling experiments were conducted using four drilling paths while changing the table movement direction and feed rate along the machining path. The accuracy of the positions of the drilled holes and condition of the drill edge after drilling were then evaluated.**

***Index Terms*—Vibration, counter balance, machine tool, DCG**

I. Introduction

In recent years, electronic devices such as mobile phones and notebook computers have become lighter, thinner, smaller, and more multifunctional. The semiconductor package substrates used in the central processing units of various electronic devices embody their advanced functions by arranging semiconductor elements on a printed circuit board and connecting circuits. Although the microfabrication of Si wafers and integrated circuit technology are improving, more sophisticated microdrilling technology for fabricating printed circuit boards by drilling holes for circuit connections is also required [1]. However, there have been few studies in this field [2] and very few reports [3] on the influence of the spinning of drills on through holes produced using tools with diameters of less than 0.2 mm.

Previous research has focused on the relationship between decreased tool heat capacity caused by reduced drill diameter and the corresponding temperature increase during processing. Drilling conditions have been considered under the constraint that a thermal alteration layer is assumed not to appear around the hole (i.e., on the hole wall surface). The method of defining these conditions has been investigated [4], but machined hole position accuracy and drill breakage prevention methods have not been investigated. Furthermore, in the current state of the industry, drilling is often performed through non-step processing using a straight drill. This is because when drilling multiple holes to form one larger hole, high-speed reciprocating motion is required in a minute area to ensure machining efficiency and the inertial force of the spindle causes vibration. However, as printed circuit board diameters become increasingly small, it is becoming clearer that in microdrilling technology, multiple-step machining can prevent chip clogging and drill breakage extremely effectively [5]. To realize this machining approach using a computer numerical control program, a drilling machine tool suitable for multiple-step machining is required.

Based on this background, a previous paper proposed a drilling machine tool equipped with a counterbalance vibration control mechanism driven by left and right ball screws and elucidated the problem of high-frequency vibration in the servo system and other components. In this study, we focused on the timing of the table feed rate changes during drilling and measured the vibration with different timings to confirm the effects on the machine tool. Drilling experiments were conducted using four different machining passes while varying the direction of table movement and feed rate. The accuracy of the positions of the drilled holes and condition of the drill edge after drilling were evaluated.

II. Experimental Device

The drilling machine tool equipped with the vibration control mechanism used in our experiment was equipped with a WESTWIND D1733 micro air drill spindle on a ND-122L numerically controlled, high-speed, single-axis drilling machine for vertical printed circuit boards manufactured by Takeuchi Co., Ltd. The experimental setup is presented in Fig. 1. The machine tool has a mechanism in which the spindle and counter are connected in series with a reverse-screw ball screw such that the counter and spindle always move in opposite directions. Consequently, the inertial force in the axial direction of the ball screw generated by the movement of the spindle is canceled by the inertial force in the axial direction of the ball screw generated by the movement of the counter. Therefore, the vibration force acting on the machine -tool housing can be suppressed. For generalization, the weight ratio is defined as $\alpha = m_C / m_S$ (where m_C [kg] is the counter weight and m_S [kg] is the spindle weight). The machine tool structure allows the weight of the counter section to be changed. Table 1 lists the specifications of the machine tool.

Manuscript received April 7, 2022; revised June 23, 2022; accepted August 23, 2022; published April 15, 2023.

Yusuke Nosaka, Toshiki Hirogaki, and Eiichi Aoyama are with Doshisha University, Japan.

*Correspondence: nosayusu411@gmail.com (Y.N.)

DOI: 10.7763/IJMO.2023.V13.825

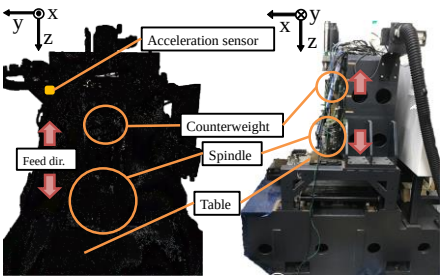

Fig. 1. Machine tool equipped with a counter balance system.

TABLE I. EXPERIMENTAL EQUIPMENT PARAMETERS

Stroke (One side) [mm]	2.6
Maximum stroke (One side) [mm]	86.0
Ball screw lead [mm]	18.0
Ball screw diameter [mm]	20.0
Weight of spindle [kg]	10.4

Fig. 2 presents the structure of the cross section. Fig. 2(a) presents the counterbalance with its center of gravity on the ball screw shaft. The weight ratio α is varied by changing the counterbalance weight mc by adding a weight compared to the state in (a). In our experiments, weights were added symmetrically such that the center of gravity of the counterbalance remained on the ball screw axis, as shown in (b). Driving the counterbalance in state (b) is called driving at the center of gravity (DCG) and its vibration reduction effect has been demonstrated using a structure that can be driven by two ball screws [6]. The acceleration of the machine tool was measured using a three-axis accelerometer at the positions shown in Fig. 1 by varying the weight ratio α. A 356B21 piezoelectric three-axis accelerometer manufactured by PCB Piezotronics was used in this experiment. The load torque of the servo motor was measured using the Sigma Win+ servo monitoring software.

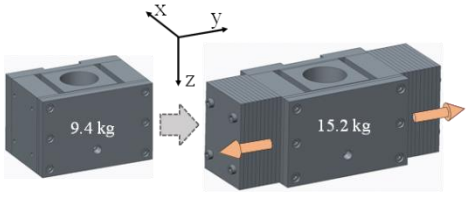

(a) m_c = 9.4 kg(DCG) (b) m_c = 15.2 kg(DCG)

Fig. 2. Construction of counter part.

III. EXPERIMENTAL METHOD

A. Vibration Measurement Experiment

The acceleration of the machine tool was measured using a three-axis acceleration sensor at the positions shown in Fig. 1 by varying the weight ratio α. The motion was a non-step motion, as shown in Fig. 3. The spindle speed was set to 240 krpm and the feed rate was set at 1920 mm/min based on the chip load of the drill used (8 μm/rev).

In our evaluation, the measured acceleration data was discrete Fourier transformed and normalized to a one-sided amplitude value. The square value of the one-sided amplitude value was then divided by the frequency resolution Δf to convert it into a value independent of the sampling conditions of the measurement. Finally, the square root of the value was taken to obtain the power spectral density (PSD). The experimental conditions are listed in Table II. In parallel, the load torque of the servo motor was measured using the Sigma Win+ servo monitoring software.

Figs. 4(a)-4(b) present the directions of table movement during the experiment. Drilling is assumed to start from point I in the +X direction operation (+XM) and +Y direction operation (+YM), and from point II in the −X direction operation (−XM) and −Y direction operation (−YM). The timing at which the table moves in parallel in a grid pattern during table operation is designated as A and the timing at which the table moves to a position displaced in the Y direction by the hole pitch from the drilling start point after drilling 100 holes is designated as B. Vibration was measured at each of these times. For measurement, B was defined as the time when the feed rate increased (after 3.2 s) during the 6.4 s acceleration measurement.

TABLE II. EXPERIMENTAL CONDITION OF THE MACHINE TOOL

Weight of spindle m_s [kg]	10.4
Weight of counterbalance m_c [kg]	9.4, 10.6, 13.5, 15.8, 18.1
Weight ratio α [-]	0.91, 1.02, 1.30, 1.52, 1.74
Feed rate v [mm/min]	1920
Number of steps	1
Hole pitch [mm]	0.35

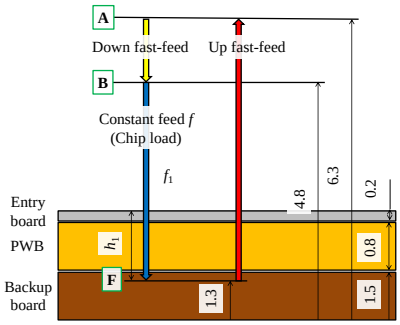

Fig. 3. Non-step drilling.

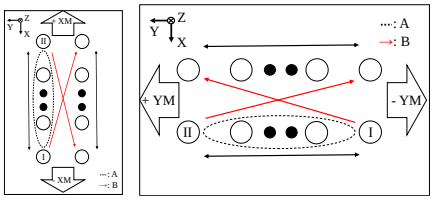

(a). ± XM (b). ± YM

Fig. 4. Table operation order.

B. Processing Experiments and Evaluation Methods

The processed specimens were FR4 double-sided copper-clad laminates (hereafter referred to as "PWBs") manufactured by Hitachi Chemical Co. The base material was epoxy resin and the reinforcing fiber was E-glass. A1050-H18 (hereafter referred to as "EB"), consisting solely of aluminum with a thickness of 0.2 mm, was used as the entry board and manufactured by Suzuka Metal Co. A 1.5-mm-thick phenolic plate PS-1160F (hereafter referred to as "BB") manufactured by Risho Kogyo was used as the backup board. Fig. 5 presents the prepared processed test specimens. The specimens were stacked in the order of EB, PWB, and BB (total thickness of 2.5 mm) from the top and machined to a depth of 1.2 mm from the top surface of the EB. Fig. 6 presents the microdrill used in this process. A carbide undercut drill manufactured by Union Tool Corp. with a

diameter of 0.15 mm and cutting length of 2.5 mm was used as the microdrill. From the perspective of drill life, a total of 3,000 holes were drilled (100 holes per row in succession). Similar to the vibration measurement experiment, the spindle speed was 240 krpm and the feed rate was 1920 mm/min in a non-step motion.

The hole position accuracy is defined as the difference between the distance between the hole position commanded by the machine tool and hole position actually machined in the X and Y directions. For the measurement of machined holes, a spindle-mounted CCD camera (800 × 600 = 480,000 pixels, 4 μm resolution) was used to capture the positions of 1000 holes in a row in groups of three and analyze the images. The centers of gravity of the pixels of the hole contours in the camera images were calculated at the NC command positions of each hole to be the center positions of the holes. The errors in X and Y between the center and NC command position for each hole are DX [μm] and DY [μm], respectively. The centers of gravity of the hole positions for 1,000 holes were determined and the errors between the centers of gravity and specified positions were defined in X and Y as DXg [μm] and DYg [μm], respectively, as shown in Fig. 7. (DX − DXg, DY − DYg) was compared for each weight ratio α to evaluate the hole position error, which eliminated the mechanical error factor. The evaluation results are presented as mean + 3s (s: standard deviation).

The direction of movement of the table varied during the experiments. Figs. 8(a) to 8(d) present the directions of table movement. Fig. 8(a) presents the machining paths used in previous research. The table is set to move from point I with the distance between holes set to 0.35 mm in the +X direction and after 100 hole drilling operations, the table moves from the drilling start point I to a position that is displaced in the Y direction by the hole pitch. Fig. 8(b) shows that after machining 100 holes, the table moves to a position displaced in the Y direction by the hole pitch from the previous position and then moves in the X direction for machining. As shown in the figure, the movement is assumed to be S-shaped. Fig. 8(c) presents the machining path that was used in a previous study, where the distance between holes is set to 0.35 mm, the table moves in the +Y direction from point I, and after 100 hole drilling operations, the table moves from the drilling start point I to a position that is shifted in the X direction by the hole pitch. Fig. 8(d) shows that after 100 hole machining operations, the table moves to a position offset in the X direction by the hole pitch from the previous position and then moves in the Y direction for machining. Subsequently, the machine is assumed to move in an S-shape, as shown in the figure.

IV. Vibration Measurement Experiment

A. Frequency Band in Drilling Operations

Consider the frequency band over which vibration is excited. Fig. 9(a) presents a graph of the motor load torque measured from inside the servomotor during the vibration measurement experiment when the table motion was +XM and the weight ratio α = 1.74. Fig. 9(b) presents a graph of the PSD calculated through frequency analysis of the torque data in Fig. 3(a). Fig. 9 (b) reveals that the frequency component of the torque is mainly below 100 Hz. Therefore, vibration modes below 100 Hz are considered to be excited during the operation of the machine tool.

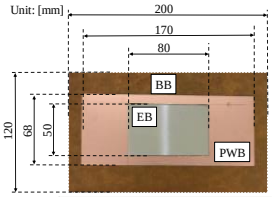

Fig. 5. Test piece for drilling.

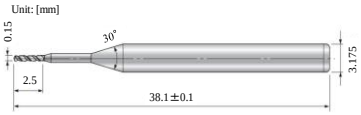

Fig. 6. Undercut drill.

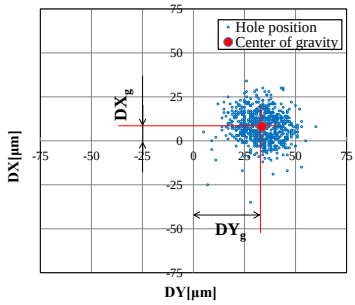

Fig. 7. Hole position error.

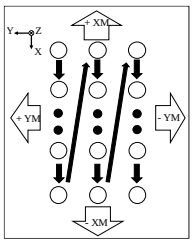

(a) Path 1

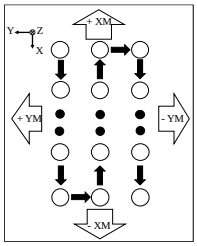

(b) Path 2

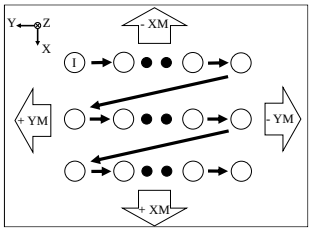

(c) Path 3

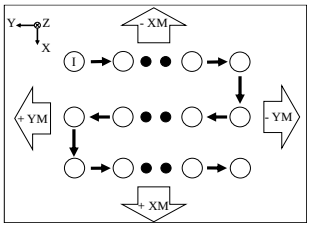

(d) Path 4

Fig. 8. Table operation order.

Fig. 10(a) presents the acceleration data (X direction) measured by the acceleration sensor at the position shown in Fig. 1 when the table motion was +XM and the weight ratio α = 1.74 in the vibration measurement experiment. Fig. 10(b) presents a graph of the calculated PSD. Fig. 10(b) reveals that the vibration components at approximately 40 and 82 Hz are relatively large, indicating that vibration modes below 100 Hz are excited.

Similarly, the acceleration in the Y direction was obtained as shown in Fig. 10(b) under conditions where the table motion was +YM and the weight ratio α = 1.74. The acceleration data (Y direction) and corresponding PSD are presented in Figs. 11(a) and 11(b), respectively. Fig. 11(b) reveals that the vibration component is relatively large at approximately 32 Hz. Based on these results, this report focuses on frequencies of approximately 32 and 82 Hz.

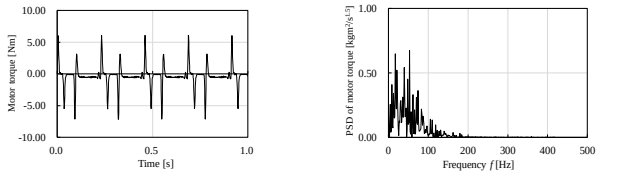

(a)Motor torque (α = 1.74) (b) PSD of motor torque (α = 1.74)

Fig. 9. Relationship between motor torque and frequency band.

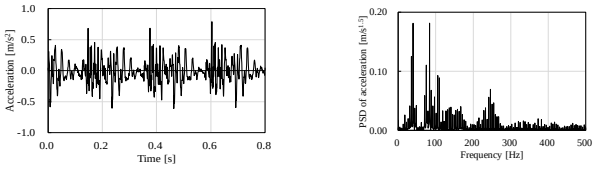

(a) Acceleration (b) PSD of acceleration

(X -direction, α = 1.74) (X -direction, α = 1.74)

Fig. 10. Relationship between acceleration and frequency band.

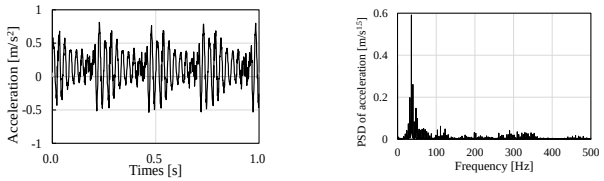

(a) Acceleration (b) PSD of acceleration

(Y -direction, α = 1.74) (Y -direction, α = 1.74)

Fig. 11. Relationship between acceleration and frequency band.

B. Finite Element Model (FEM) and Natural Frequency

An FEM was used to simulate the vibration characteristics in the X and Y directions. Fig. 12(a) presents the FEM. Using this model, eigenvalue analysis was conducted to confirm the vibration modes at approximately 82 Hz, as shown in Fig. 12(b). This vibration is considered to be caused in the X direction by deformation of the support section of the machine tool. This is referred to as the bending vibration mode. The vibration mode at approximately 32 Hz is presented in Fig. 12(c). This is considered to be a vibration in the Y direction caused by tilting as a result of deformation of the ground, rather than deformation of the machine tool itself. This is referred to as the rocking vibration mode.

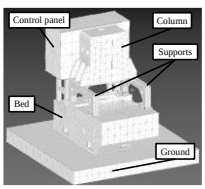

(a) Before transformation

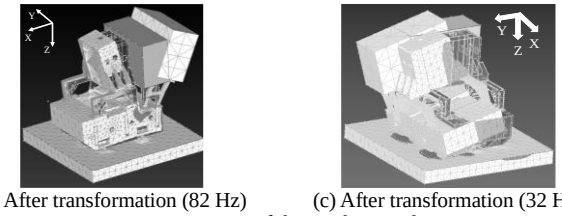

(b) After transformation (82 Hz) (c) After transformation (32 Hz)

Fig. 12. FEM of the machine tool.

C. Results and Discussion

Based on the results of eigenvalue analysis, we measured the vibrations at approximately 82 and 32 Hz. Figs. 13(a) to 13(d) present the relationship between the PSD in the X direction at approximately 82 Hz, PSD in the Y direction at approximately 32 Hz, and weight ratio α, respectively, obtained from the vibration measurement experiments at timings A and B for the table movement directions shown in Figs. 4(a) and 4(b). Figs. 4(a) and 4(b) reveal that in both table movement directions, vibration increases at timing B, where the feed rate is greater than that at timing A and the tables are moving in parallel in a grid pattern. In a previous study, drilling experiments were conducted using the machining path shown in Fig. 4 to measure positional accuracy.

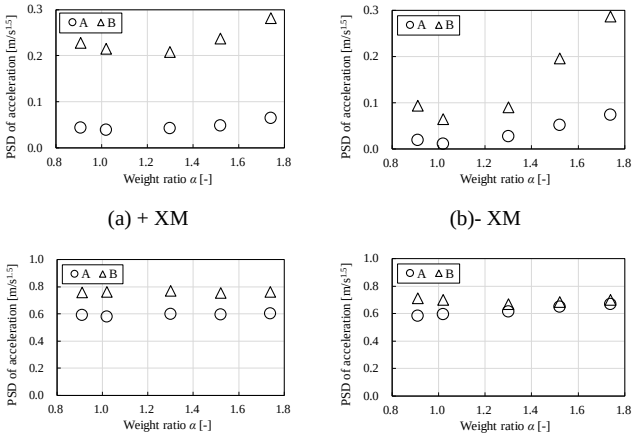

(a) + XM (b)- XM

(c) + YM (d) - YM

Fig. 13. Relationship between PSD of acceleration and weight ratio α.

V. Processing Experiment and Discussion

A. Hole Position Accuracy

This section presents comparisons of the measured hole positional accuracy results from actual machining experiments using Paths 1 to 4. Fig. 14 presents the hole position error for each weight ratio in each machining pass. Fig. 14 reveals that the accuracy of Paths 2 and 4, which move in an S-shape, changes significantly when the weight ratio α = 1.30, whereas the errors remain consistent for the other weight ratios. Fig. 15 presents the hole positioning accuracy for each weight ratio when the table is moved in four directions (±XM, ±YM) in a grid pattern, corresponding to Paths 1 and 3. Fig. 15 reveals that the hole position error is minimized when the table is moved in the −X direction. Because Path 2 is the only machining path in which the table moves by 100 holes in the −X direction, this movement is considered to have a significant effect on the hole position accuracy. The same trend based on the effect of the weight ratio can be observed in Figs. 13(a) and 13(b), where the X-directional vibration is reduced at α = 1.02, suggesting that the hole position accuracy is more affected by X-directional vibration than Y-directional vibration.

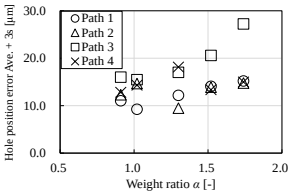

Fig. 14. Relationship between hole position error Ave. +3s and weight ratio α.

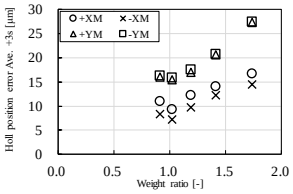

Fig. 15. Relationship between hole position error Ave. + 3s and weight ratio α.

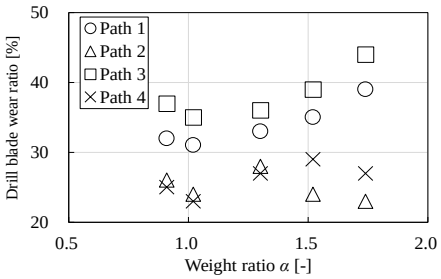

Fig. 17. Relation between drill blade loss ratio and weight ratio α.

B. Drill Blade Surface

Following the machining experiments, the cutting edges of the drills were observed using a microscope to evaluate the chipping and wear on the drill relief surface and compare drill life. The table was operated in the machining path shown in Fig. 8 with a distance of 0.35 mm between holes and the drill cutting edges used in the machining experiments are presented in Fig. 16 for Path 1. Based on the observed drill cutting edge surface, the loss area of the cutting edge surface divided by the area of unused drill cutting edge surface expressed as a percentage is the loss rate. The loss rate of the cutting edge surface when the table is operated in each machining pass is presented in Fig. 17. Fig. 17 reveals that the loss rate is lower for Paths 2 and 4, which move in an S-shape, than for Paths 1 and 3, which have a timing where the feed rate increases. Compared to the hole position accuracy shown in Fig. 14, the hole position accuracy changes significantly for Paths 2 and 4 with α = 1.02 and 1.30, but it is difficult to conclude that the accuracy is better than that of Path 1. Therefore, a machining path with a unified table feed rate that moves in an S-shape reduces vibration and motion. However, the effect on hole position accuracy is small and only the surface of the drill edge is significantly affected.

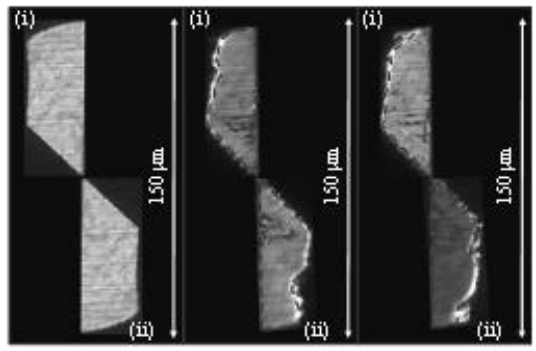

(a) Unused (b) α = 0.91 (c) α = 1.02

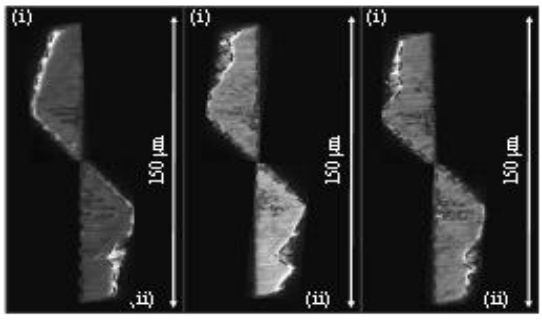

(d) α = 1.30 (e) α = 1.52 (f) α = 1.74

Fig. 16. Face of the drill edge.

VI. Conclusion

In this report, focusing on the timing of table feed rate changes during drilling, drilling experiments were conducted using four drilling paths while changing the table movement direction and feed rate along the machining path. The accuracy of the positions of the drilled holes and condition of the drill edge after drilling were evaluated. The following findings were obtained:

1. The vibration generated by drilling in the –X -direction with S-shaped table motion can be significantly reduced, but the effect of changes in the weight ratio is small.

2. A machining path with a uniform table feed rate that moves in an S-shape reduces vibration and motion, but the effect on hole positional accuracy is small, and only the surface of the drill edge is considered to be significantly affected.

Conflict of Interest

The authors declare no conflict of interest.

Author Contributions

All authors (1) made substantial contributions to the study concept or the data analysis or interpretation; (2) drafted the manuscript or revised it critically for important intellectual content; (3) approved the final version of the manuscript to be published; and (4) agreed to be accountable for all aspects of the work.

References

[1] H. Shi, X. Liu, and Y. Lou, "Materials and micro drilling of high frequency and high speed printed circuit board: A review," *The International Journal of Advanced Manufacturing Technology*, vol. 29, no. 100, 2019, pp. 827-841.

[2] J. S. Moon, H. S. Yoon, G. B. Lee, and S. H. Ahn, "Effect of backstitch tool path on micro-drilling of printed circuit board," *Precision Engineering*, vol. 38, no. 3, 2014, pp. 691-696.

[3] H. Watanabe, H. Tsuzaka, and M. Masuda, "Microdrilling for printed circuit boards (PCBs) — Influence of radial run-out of microderills on hole quality," *Precision Engineering*, vol. 32, no. 4, 2008, pp. 329–335.

[4] T. Hirogaki, E. Aoyama, K. Ogawa, T. Otsuka, and H. Nojiri, "Study on thermal damage of micro diameter hole drilled by super-high-speed spindle in PWB and optimum drilling condition," *Transactions of the Japan Society of Mechanical Engineers*, vol. 74, no. 743, 2008, pp. 1894–1900.

[5] T. Hirogaki, E. Aoyama, T. Yamashita, M. Kishimoto, and Y. Kawazoe, "Fundamental study on machine tools equipped with vibration suppression mechanism based on left and right ball screw and with an ultra-high-speed spindle for micro-drilling," *Transactions of the Japan Society of Mechanical Engineers*, vol. 83, no. 850, 2017.

[6] K. Hiramoto, A. Hansel, S. Ding, and K. Yamazaki, "A study on the drive at center of gravity (DCG) feed principle and its application for

development of high-performance machine tool systems," *CIRP Annals*, vol. 54, no. 1, 2005, pp. 333-336.

Yusuke Nosaka was born in 1998 in Osaka, Japan. He attended Doshisha University (Japan) for his undergraduate studies and obtained his B.S. in science and engineering in 2021.

He is currently enrolled in a doctoral program in the Graduate School of Science and Engineering at Doshisha University. Currently, he is conducting research using drilling machine tools equipped with counterbalance vibration control mechanisms.

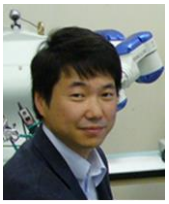

Toshiki Hirogaki is a professor of faculty of science and engineering Doshisha University in Kyoto, Japan. He received his the B.S., M.S. and Ph.D. degrees in mechanical engineering from Doshisha University in Kyoto, Japan in 1988, 1990 and 1994. His major is manufacturing and automation technology.

Eiichi Aoyama is a professor of faculty of science and engineering Doshisha University in Kyoto, Japan. He received his the B.S., M.S. and Ph.D. degrees in mechanical engineering from Doshisha University in Kyoto, Japan in 1976, 1978 and 1993. His major is advanced process technology.